Korean J. Chem. Eng., 34(12), 3132-3141 (2017)
DOI: 10.1007/s11814-017-0229-4

pISSN: 0256-1115
eISSN: 1975-7220

Deep desulfurization of model oil by photocatalytic air oxidation and adsorption using $Ti_{(1-x)}M_xO_2$ (M=Zr, Ce)

Wei Zhang*,, Xin Li*,***, Hong Wang*,**, Yongji Song*,**, Shenghong Zhang*, and Cuiqing Li*,**,†**

*School of Chemical Engineering, Beijing Institute of Petrochemical Technology, Beijing 102617, P. R. China
**Beijing Key Laboratory of Fuels Cleaning and Advanced Catalytic Emission Reduction Technology, Beijing 102617, P. R. China
***School of Chemical Engineering, Beijing University of Chemical Engineering, Beijing 100029, P. R. China
(*Received 6 March 2017 • accepted 15 August 2017*)

Abstract−Deep desulfurization of model oil by photocatalytic air oxidation and adsorption using $Ti_{(1-x)}M_xO_2$ (M=Zr, Ce) was investigated. $Ti_{(1-x)}M_xO_2$ (M=Zr, Ce) was prepared by urea gelation/co-precipitation method, and characterized by N_2 adsorption, XRD and UV-vis spectra. UV irradiation greatly enhanced the adsorptive capacity and selectivity of TiO_2-ZrO_2 for organosulfur in model oil because organosulfur compounds were first photocatalytically oxidized to sulfoxides and sulfones over TiO_2-ZrO_2, which were then selectively adsorbed on the bifunctional material due to much higher polarities of generated sulfoxides and sulfones. The Ti/Zr molar ratio and calcination temperature were optimized to 5 : 5 and 500 °C with the sulfur removal of 99.6% after reaction for 2 h under UV irradiation. After adding 25 wt% toluene into model oil, the sulfur removal could still reach 97.2% after reaction for 7 h. TiO_2-ZrO_2 could be well regenrated by washing with acetonitrile followed by thermal treatment in air.

Keywords: Adsorptive Desulfurization, Photocatalysis, Dibenzothiophene, Selectivity, TiO_2-ZrO_2

INTRODUCTION

SO_x generated upon combustion of sulfur-containing diesel fuel contributes to acid rain, and also the emission of harmful particulate matter (PM) in vehicle exhaust. Therefore, the sulfur content in diesel fuel has been regulated to be a maximum of 15 ppmw or 10 ppmw in many developed countries [1]. Furthermore, the development of fuel cells calls for the production of ultra-low-sulfur diesel (<1 ppmw-S). Diesel fuel is a promising feedstock for fuel cells due to its high energy density. However, more than 1 ppmw sufur in diesel poisons the fuel processing catalysts and fuel cell electrodes. Consequently, ultra-deep desulfurization of diesel fuel has gained much attention. Currently, hydrodesulfurization (HDS) is the major desulfurization process in petroleum refineries operating at high temperatures (320-380 °C) and high pressure (3-7 MPa) using large amounts of hydrogen. However, it is difficult or costly to produce ultra-low-sulfur diesel by employing HDS process because of low reactivity of the refractory dibenzothiophene and alkyl substituted dibenzothiophenes due to their steric hindrance effects [2]. Therefore, developing alternative desulfurization approaches to ultra-deep desulfurization of diesel fuel is highly desirable.

Adsorptive desulfurization (ADS), which employs adsorbents to selectively remove organosulfur compounds in diesel fuel, is one of the most promising alternative approaches due to its capability of ultra-deep desulfurization under ambient conditions [3]. In recent years, efforts have been made to develop efficient adsorbents for ultra-deep desulfurization, including carbon materials [4], zeolites [5], metal organic frameworks (MOFs) [6], surface molecularly imprinted polymers (SMIP) [7]. However, most of the adsorbents are not effective for adsorptive desulfurization of real diesel fuel due to the competitive adsorption of a relatively large amount of aromatics with the coexisting organosulfur compounds with the similar aromatic skeleton structure. Bhandari et al. [8] investigated the effect of aromatics on the adsorptive desulfurization capacity of Ni-Y zeolite, and indicated that the breakthrough capacity of 4,6-dimethyldibenzothiophene (4,6-DMDBT) on Ni-Y zeolite dramatically decreased from 400 cm^3-fuel/g-adsorbent to zero with increasing the aromatic content in model diesel from zero to 25% (v/v). To improve the ADS selectivity, some researchers have carried out reactive adsorption desulfurization over bifunctional materials in the presence of an oxidant. Ma et al. [9] prepared $Fe(NO_3)_3$ and $FeBr_3$ co-loaded activated carbon (Fe-Fe/AC) for reactive adsorption desulfurization in the presence of oxygen under ambient conditions, and reported that the conversion of the organosulfur compounds to their corresponding sulfones and/or sulfoxides over Fe-Fe/AC significantly improved the adsorptive selectivity of the organosulfur compounds on activated carbon due to the much higher polarity of the formed sulfones and sulfoxides than the original organosulfur compounds. Ren [10] investigated catalytic adsorptive desulfurization (CADS) of model diesel fuel using TiO_2/SBA-15 as the bifunctional material and cumene hydroperoxide as the oxidant under mild conditions, and found that desulfurization uptake by TiO_2/SBA-15 under CADS was two-magnitudes higher than that under ADS without the in-situ catalytic oxidation of dibenzothiophene due to the oxidation of DBT to $DBTO_2$ over TiO_2/SBA-15 by cumene hydroperoxide. These findings suggest that the

†To whom correspondence should be addressed.
E-mail: licuiqing@bipt.edu.cn

desulfurization selectivity could be facilitated by synergic effect of catalytic oxidation and adsorption over a bifunctional material.

Given that photocatalysis is an advanced oxidation technology via which molecular oxygen (O_2) can be activated to superoxide anion (O_2^-) [11,12], which might selectively attack organosulfur compounds to form sulfoxide or sulfones since the sulfur atom on organosulfur compounds has two unpaired electrons, it is expected that porous photocatalysts with high surface area might act as the bifunctional materials for synergistic photocatalytic-adsorptive desulfurization under light irradiation. Attributed to its high photocatalytic ability, nontoxicity, chemical stability and low cost, TiO_2 was the most widely studied photocatalyst in the last decades [13, 14]. However, pure TiO_2 usually has relatively low quantum efficiency and low surface area. It has been reported that coupling TiO_2 with ZrO_2 or CeO_2 will lead to an increase in the photocatalytic ability and surface area [15,16].

In this work, a series of bifunctional $Ti_{(1-x)}M_xO_2$ (M=Zr, Ce) materials were developed and examined for synergistic photocatalytic-adsorptive desulfurization of model oils. The sulfur species during photocatalytic reaction were identified by GC-MS, and a pathway of synergistic photocatalytic-adsorptive desulfurization was proposed. The $Ti_{(1-x)}M_xO_2$ (M=Zr, Ce) composites were characterized by N_2 adsorption-desorption, X-ray diffraction (XRD) and UV-vis diffuse reflectance spectroscopy. The effect of Ti/Zr ratio in $Ti_{(1-x)}Zr_xO_2$ composites, its calcination temperature and fuel-to-adsorbent weight ratio on the synergistic photocatalytic-adsorptive desulfurization performance were investigated. The reactivity of various organosulfur compounds and the effect of aromatics in diesel fuel on the synergistic photocatalytic-adsorptive desulfurization selectivity were discussed. In addition, the regeneration of TiO_2-ZrO_2 was further investigated.

EXPERIMENTAL

1. Materials

Benzothiophene (BT, 97%), Dibenzothiophene (DBT, 98%) and 4,6-dimethyldibenthiophene (4,6-DMDBT, 97%) were purchased from Aladdin Reagent Co., Ltd. Titanium tetrachloride ($TiCl_4$, 99.9%), cerium ammonium nitrate $(NH_4)_2Ce(NO_3)_6$ (99%), zirconium(IV) oxynitrate hydrate $ZrO(NO_3)_2{\cdot}xH_2O$ (99%), acetone, dodecane and urea (99%) were supplied by Tianjing Guangfu Science & Technology Development Co., Ltd., China.

The model oils with a sulfur content of 50 ppmw were prepared by dissolving BT, DBT or 4, 6-DMDBT into dodecane, respectively. A model oil containing 500 ppmw S was also prepared to represent relatively high-sulfur model oil. In addition, the model oil containing 25 wt% toluene was prepared by dissolving DBT into the mixed solution (25 wt% toluene in 75 wt% dodecane) to investigate the synergistic photocatalytic-adsorptive desulfurization selectivity.

2. Preparation of $Ti_{(1-x)}M_xO_2$ (M=Zr, Ce) Metal Oxides

A series of $Ti_{(1-x)}Zr_xO_2$ mixed oxides (x=0, 0.1, 0.3, 0.5, 0.7, 0.9, 1.0) were prepared by urea gelation/co-precipitation method [17]. $TiCl_4$ and $ZrO(NO_3)_2{\cdot}xH_2O$ with a pre-determined Ti/Zr molar ratio were dissolved in deionized water, and then excess urea were added. The molar ratio of $TiCl_4$: $ZrO(NO_3)_2{\cdot}xH_2O$: urea was (1−x) : x : 8. The solution was heated to 90-95 °C and maintained at this temperature range until the pH value of the solution reached 6.0. After that, the solution was aged for 0.5 h and then filtered. The obtained precipitate was dried overnight in an oven at 110 °C and calcined at different temperatures for 4 h, respectively. The obtained $Ti_{(1-x)}Zr_xO_2$ metal oxides with varied Ti/Zr molar ratios calcined at 500 °C were labeled as $Ti_{(1-x)}Zr_xO_2$-500. $Ti_{0.5}Zr_{0.5}O_2$ calcined at 300 °C, 400 °C, 500 °C, 600 °C and 700 °C was labeled as $Ti_{0.5}Zr_{0.5}O_2$-300, $Ti_{0.5}Zr_{0.5}O_2$-400, $Ti_{0.5}Zr_{0.5}O_2$-500, $Ti_{0.5}Zr_{0.5}O_2$-600, $Ti_{0.5}Zr_{0.5}O_2$-700, respectively.

$Ti_{0.5}Ce_{0.5}O_2$-500 was also prepared following the same procedure and calcined at 500 °C for 4 h.

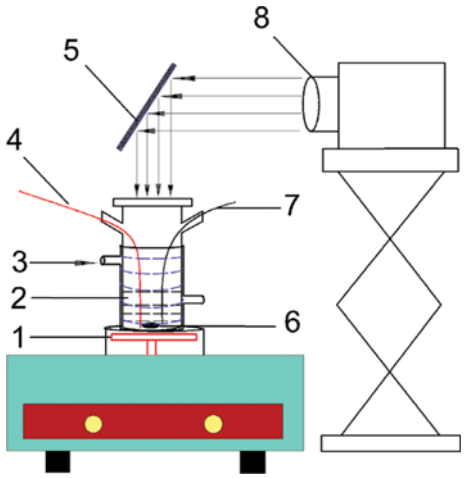

Fig. 1. Schematic diagram of the experimental apparatus of synergistic photocatalytic-adsorptive desulfurization.

1. Magnetic stirrer	5. UV reflector
2. Model diesel fuel	6. Stirrer bar
3. Water bath	7. Sampling port
4. Air inlet	8. Xenon lamp

3. Desulfurization Experiments

Desulfurization experiments with/without UV irradiation were conducted in a photochemical reactor (CEL-HXUV300E, Beijing Zhongjiaojinyuan Co., Ltd., China) (Fig. 1). The reaction system consists of a 300 W xenon lamp with an ultraviolet reflection filter as the light source, a circulator bath to control the temperature, a 100 mL three-mouth glass reactor and a magnetic stirrer. Since all reactions in our work were conducted at room temperature of 25 °C, the condenser was not included in the reactor, and the evaporation losses were within 2% after reaction for 7 h with the air flow rate of 40 ml/min.

In a typical run, 10 g of model oil and 0.5 g of the adsorbent were added in the reactor and molecular oxygen was bubbled at the flow rate of 40 ml/min through the reaction solution simultaneously. The mixture was kept at 25 °C by a circulator bath throughout the experiment. Before irradiation, the mixture was stirred vigorously in the dark for 1 h to attain adsorption-desorption equilibrium and then it was irradiated by the UV light for 7 h. The mixture was sampled periodically and filtered before analysis. 0.5 g of the spent $Ti_{0.5}Zr_{0.5}O_2$-500 after irradiation for 1 h was washed with 5 ml of acetone, and the eluent was also analyzed by GC-MS to identify the sulfur species adsorbed on the composite.

4. Analysis of the Treated Fuel Samples

4-1. Quantitative Analysis of Organosulfur Compounds and Toluene

The sulfur and toluene contents of the model oils were analyzed by a gas chromatograph (agilent-7890B) equipped with a flame ionization detector coupled with a sulfur chemiluminescence detector (Sievers-355) (GC-FID-SCD). The GC was equipped with a DB-Sulfur capillary column (40 m×0.32 mm×0.75 μm), using highly purified nitrogen (≥99.9995 wt%) as the carrier gas. The injector temperature was set at 260 °C, and the injection volume of 1.5 μl and a split ratio of 20 was used. The initial oven temperature was set at 150 °C for 1 min and was then increased to 250 °C at a heating rate of 20 °C·min^{-1}, and held at 250 °C for 5 minutes.

4-2. Identification of Oxidation Product of DBT

The oxidation product of dibenzothiophene was identified by gas chromatogram-mass spectrometry (GC-MS) (Agilent 7890B/5977A) equipped with a HP-5ms capillary column (30 m×0.25 mm ×0.25 μm). Analysis conditions were as follows: injection port temperature, 275 °C; split ratio, 1/50; injection volume of sample, 0.2 μl; column flow rate, 1 mL/min; the oven temperature was programmed with the initial temperature of 120 °C, increased to 180 °C at 10 °C/min, held for 2 minutes, and then increased to 250 °C at 2 °C/min and held for 1 min.

5. Characterization

5-1. Textural Analysis

Textural properties of the $Ti_{(1-x)}M_xO_2$ (M=Zr, Ce) metal oxides were characterized by N_2 adsorption-desorption isotherms at 77 K by using a Micromeritics ASAP2020 surface area and porosimetry analyzer. Prior to textural analysis, the sample was degassed under vacuum at 250 °C for 8 h. The specific surface areas were evaluated from the adsorption isotherms using the Brunauer-Emmett-Teller (BET) equation in the p/p_0 range of 0.05-0.2. The average pore size was evaluated from the adsorption branch of the isotherm using the BJH model. The total pore volume was estimated by a single point method at p/p_0=0.99.

5-2. UV-vis Diffuse Reflectance Spectra

UV-vis diffuse reflection spectra were recorded on a UV-vis spectrometer (TU-1950, Beijing Purkinje General Instrument Co., Ltd., China) in the wavelength range of 200-800 nm using $BaSO_4$ as the reflectance standard material.

Table 1. Textural properties of various $Ti_xZr_{(1-x)}O_2$ and $Ti_{0.5}Ce_{0.5}O_2$-500

Catalysts	BET surface area (m^2/g)	Average pore size (nm)	Total pore volume (m^3/g)
TiO_2-500	98.6	8.10	0.2328
$Ti_{0.9}Zr_{0.1}O_2$-500	141.3	10.56	0.4888
$Ti_{0.7}Zr_{0.3}O_2$-500	151.2	9.61	0.3129
$Ti_{0.5}Zr_{0.5}O_2$-500	256.4	3.44	0.2652
$Ti_{0.3}Zr_{0.7}O_2$-500	231.5	3.25	0.2011
$Ti_{0.1}Zr_{0.9}O_2$-500	227.3	2.94	0.1642
ZrO_2-500	78.1	3.18	0.0613
$Ti_{0.5}Zr_{0.5}O_2$-400	300.1	3.84	0.3522
$Ti_{0.5}Zr_{0.5}O_2$-600	186.2	4.85	0.2858
$Ti_{0.5}Zr_{0.5}O_2$-700	66.9	13.92	0.2439
$Ti_{0.5}Ce_{0.5}O_2$-500	126.4	5.71	0.2422

5-3. X-ray Diffraction (XRD) Analysis

Powder X-ray diffraction (XRD) patterns of the catalysts were obtained on a SHIMADZU XRD-7000 powder diffractometer using Cu Kα radiation at a scanning rate of 4°·min^{-1} from 10° to 90°.

RESULTS AND DISCUSSION

Table 1 lists the textural properties of $Ti_xZr_{(1-x)}O_2$-500 with varied Ti/Zr molar ratios, $Ti_{0.5}Zr_{0.5}O_2$ calcined at different temperatures as well as $Ti_{0.5}Ce_{0.5}O_2$-500. The data in Table 1 indicates that various $Ti_xZr_{(1-x)}O_2$ showed the mesoporous stucture at the average pore sizes of 3-14 nm. For various $Ti_xZr_{(1-x)}O_2$-500, TiO_2-ZrO_2 mixed oxides exihibited higher surface area than TiO_2 and ZrO_2 single oxides. In particular, $Ti_{0.5}Zr_{0.5}O_2$-500 exhibited the highest surface area of 256.4 m^2/g among various $Ti_xZr_{(1-x)}O_2$-500. For various $Ti_{0.5}Zr_{0.5}O_2$ calcined at different temperatures, the surface area of $Ti_{0.5}Zr_{0.5}O_2$ decreased with increasing the calcination temperature. Compared to $Ti_{0.5}Zr_{0.5}O_2$, $Ti_{0.5}Ce_{0.5}O_2$-500 had much lower surface area of 126.4 m^2/g.

Fig. 2 shows the XRD spectra of various $Ti_xZr_{(1-x)}O_2$-500 with varying Ti/Zr ratios (Fig. 2(a)) and $Ti_{0.5}Zr_{0.5}O_2$ calcined at different temperatures (Fig. 2(b)). In Fig. 2(a), TiO_2 shows clear characteris-

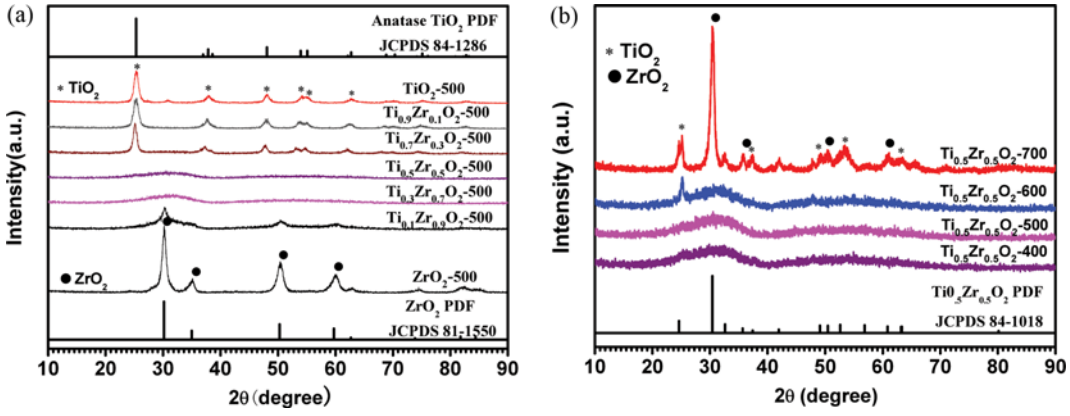

Fig. 2. (a) XRD patterns of various $Ti_xZr_{(1-x)}O_2$-500, (b) XRD patterns of various $Ti_{0.5}Zr_{0.5}O_2$ calcined at different temperatures.

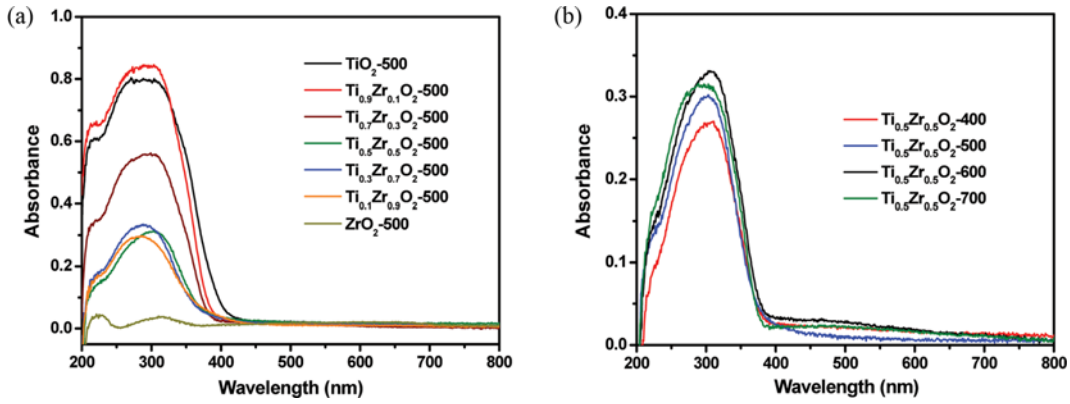

Fig. 3. (a) UV-vis diffuse reflectance spectra of ZrO_2-500, TiO_2-500 and various $Ti_xZr_{(1-x)}O_2$-500, (b) UV-vis diffuse reflectance spectra of various $Ti_{0.5}Zr_{0.5}O_2$ calcined at different temperatures.

tic peaks at 25.28°, 37.80°, 48.05°, 53.89°, 55.06°, 62.88°, which correspond to anatase phase (101), (004), (200), (105), (211), (213) reflections in agreement with the JCPDS pattern of anatase TiO_2 (84-1286), suggesting TiO_2-500 was present in the anatase phase. With the incorporation of ZrO_2 into TiO_2, the characteristic peaks of TiO_2 gradually decrease, indicating a decrease in the particle size of TiO_2 due to the dissimilar nuclei, coordination geometry and an increase in the surface area [18]. Meanwhile, no obvious characteristic peaks of ZrO_2 appear until the Zr/Ti reaches 7 : 3, suggesting ZrO_2 is well dispersed in TiO_2 when the Zr/Ti ratio in $Ti_xZr_{(1-x)}O_2$-500 is lower than 7 : 3. As the Zr/Ti ratio in $Ti_xZr_{(1-x)}O_2$-500 continues to increase, the characteristic peaks of ZrO_2 appear and increase gradually, which matches with the JCPDS pattern of ZrO_2 (81-1550). However, no characteristic peaks of TiO_2 appear when the Zr/Ti ratio in $Ti_xZr_{(1-x)}O_2$-500 is higher than 5 : 5, suggesting TiO_2 is well dispersed in ZrO_2 in the case of the Zr/Ti ratio in $Ti_xZr_{(1-x)}O_2$-500 higher than 5 : 5.

Fig. 2(b) illustrates the XRD spectra of various $Ti_{0.5}Zr_{0.5}O_2$ calcined at different temperatures. It was visible that no characteristic peaks of ZrO_2 or TiO_2 in $Ti_xZr_{(1-x)}O_2$ appeared at the calcination temperature range of 400 °C-500 °C, while the characteristic peaks of ZrO_2 or TiO_2 appeared at the calcination temperature of 600 °C, and the intensity of peaks sharply increased with increasing calcination temperature from 600 °C to 700 °C, indicating the crystalline sizes of ZrO_2 or TiO_2 increased with calcination temperature. Moreover, the characteristic peaks of $Ti_{0.5}Zr_{0.5}O_2$-700 agreed well with the JCPDS pattern of $Ti_{0.5}Zr_{0.5}O_2$ (84-1018).

Fig. 3 shows UV-vis diffuse reflectance spectra of various $Ti_xZr_{(1-x)}O_2$-500 with varying Ti/Zr ratios (Fig. 3(a)) and $Ti_{0.5}Zr_{0.5}O_2$ calcined at different temperatures (Fig. 3(b)). In Fig. 3(a) most of the TiO_2-ZrO_2 mixed oxides exhibit lower UV absorption than single TiO_2, but higher adsorption than single ZrO_2. Fig. 3(b) illustrates UV-vis diffuse reflectance spectra of $Ti_{0.5}Zr_{0.5}O_2$ calcined at different temperatures. UV absorption of $Ti_{0.5}Zr_{0.5}O_2$ increased with increasing calcination temperature from 400 °C to 600 °C, and then decreases slightly when the calcination temperature is further increased to 700 °C.

1. Adsorption of Organosulfur Compounds over $Ti_{0.5}Zr_{0.5}O_2$-500 and $Ti_{0.5}Ce_{0.5}O_2$-500

Fig. 4 shows the adsorption kinetics of DBT over $Ti_{0.5}Zr_{0.5}O_2$-500 and $Ti_{0.5}Ce_{0.5}O_2$-500 from 50 ppmw-S model oil at 298 K. Adsorption equilibrium of DBT was attained in about 30 min over

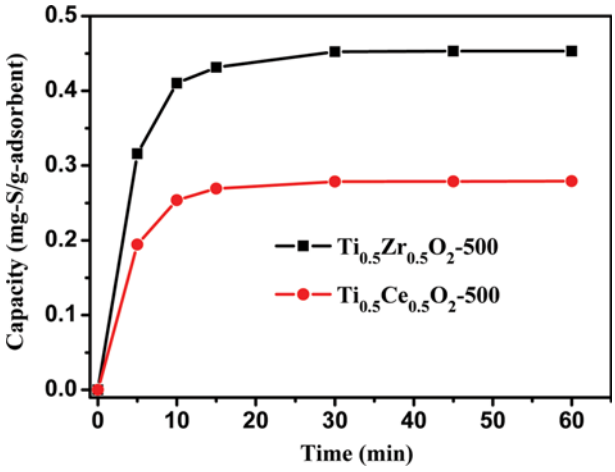

Fig. 4. Adsorption kinetics of DBT over $Ti_{0.5}Zr_{0.5}O_2$-500 and $Ti_{0.5}Ce_{0.5}O_2$-500 from 50 ppmw-S model oil at 298 K.

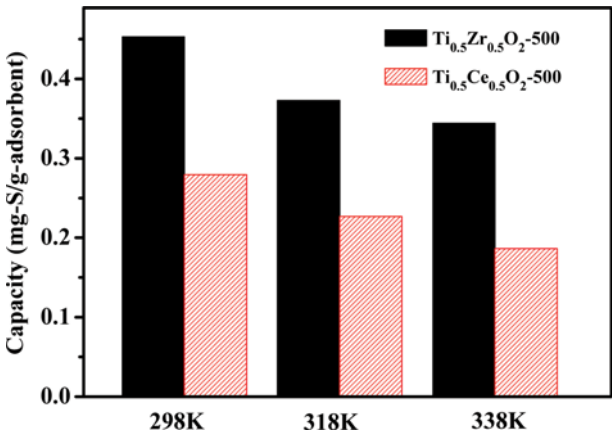

Fig. 5. Effect of temperature on adsorption capacities of DBT over $Ti_{0.5}Zr_{0.5}O_2$-500 and $Ti_{0.5}Ce_{0.5}O_2$-500 from 50 ppmw-S model oil.

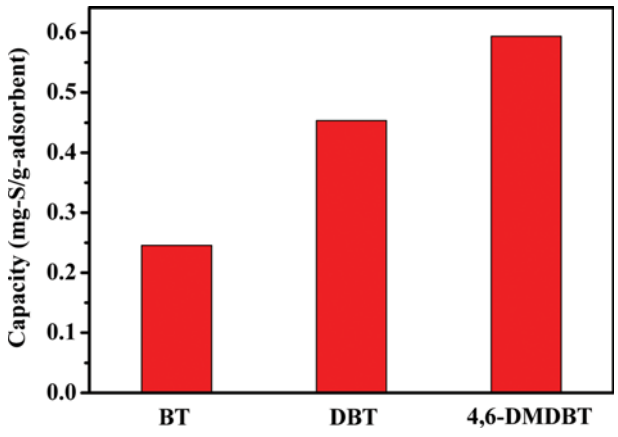

Fig. 6. Adsorption capacity of $Ti_{0.5}Zr_{0.5}O_2$-500 for various organosulfur compounds from 50 ppmw-S model oils at 25 °C.

both $Ti_{0.5}Zr_{0.5}O_2$-500 and $Ti_{0.5}Ce_{0.5}O_2$-500. $Ti_{0.5}Zr_{0.5}O_2$-500 showed the higher equilibrium adsorption capacity of 0.45 mg/g than $Ti_{0.5}Ce_{0.5}O_2$-500, over which 0.28 mg/g of adsorption capacity was reached. The reason may be that $Ti_{0.5}Zr_{0.5}O_2$-500 had higher surface area than $Ti_{0.5}Ce_{0.5}O_2$-500.

Fig. 5 shows the DBT adsorption capacities of $Ti_{0.5}Zr_{0.5}O_2$-500 and $Ti_{0.5}Ce_{0.5}O_2$-500 at 298, 318, 338 K. Adsorption capacity of DBT decreased with increasing adsorption temperature over both $Ti_{0.5}Zr_{0.5}O_2$-500 and $Ti_{0.5}Ce_{0.5}O_2$-500, indicating low adsorption temperature was preferred.

Fig. 6 presents adsorption capacities of $Ti_{0.5}Zr_{0.5}O_2$-500 for various organosulfur compounds. The adsorptive selectivity of $Ti_{0.5}Zr_{0.5}O_2$-500 for different organosulfur compounds followed the order of 4,6-DMDBT>DBT>BT. The alkyl groups on organosulfur molecule increased the adsorptive capacity, probably because the adsorption of sulfur compounds might occur through the interactions between π electrons in the thiophenic aromatic ring structure and the surface of $Ti_{0.5}Zr_{0.5}O_2$-500 [19,20], and the alkyl group was an electron donator, which enhanced the electron density of aromatic ring [21,22].

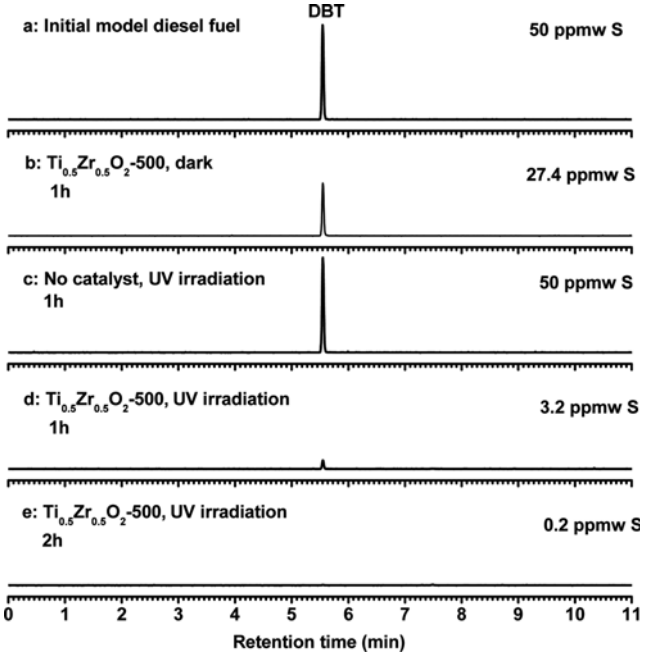

Fig. 7. SCD chromatograms of model oils treated with/without the UV light irradiation and $Ti_{0.5}Zr_{0.5}O_2$-500.

2. Synergistic Photocatalytic-adsorptive Desulfurization of Model Oil

Desulfurization experiments with/without UV light irradiation and $Ti_{0.5}Zr_{0.5}O_2$-500 were conducted with air bubbling in a batch reactor at 25 °C, and SCD chromatograms of treated model oils are shown in Fig. 7. Fig. 7(a) shows the SCD chromatogram of original model diesel fuel. The representative organosulfur compound in initial model diesel fuel was DBT and the sulfur content was 50 ppmw. In Fig. 7(b) after treatment with $Ti_{0.5}Zr_{0.5}O_2$-500 in the dark for 1 h, the sulfur content of model oil was reduced to 27.4 ppmw with the sulfur removal of 45.2%, which was attributed to the adsorption of DBT on $Ti_{0.5}Zr_{0.5}O_2$-500. Fig. 7(c) shows that after the initial model oil was treated by UV irradiation in the absence of $Ti_{0.5}Zr_{0.5}O_2$-500, no new sulfur species were formed in the UV-treated fuel and the sulfur content did not decrease, indicating that organosulfur in model oil could not be oxidized in the presence of UV irradiation but without a photocatalyst. It is clearly visible from Fig. 7(d) that after reaction in the presence of both UV irradiation and $Ti_{0.5}Zr_{0.5}O_2$-500 for 1 h, the sulfur content in model oil decreased sharply from 50 ppmw to 3.2 ppmw with the sulfur removal of 93.6%, which was 48.4% higher that that in the presence of $Ti_{0.5}Zr_{0.5}O_2$-500 but without UV irradiation, suggesting the strong promotion effect of UV irradiation on the desulfurization capacity of $Ti_{0.5}Zr_{0.5}O_2$-500. Furthermore, after reaction for 2 h, the sulfur removal reached nearly 100%, as shown in Fig. 7(e).

The adsorption capacity of an adsorbent for a substance depends on the surface characteristics of the adsorbent as well as the nature of the substance. Based on the fact that UV irradiation greatly enhanced the adsorptive capacity of $Ti_{0.5}Zr_{0.5}O_2$-500 for DBT, we hypothesized that DBT was converted to other sulfur spices in the presence of both UV irradiation and $Ti_{0.5}Zr_{0.5}O_2$-500. However, no new species were detected in the treated fuels in the presence of UV irradiation and $Ti_{0.5}Zr_{0.5}O_2$-500 (Fig. 7(d) and Fig. 7(e)). Afterwards, the spent $Ti_{0.5}Zr_{0.5}O_2$-500 was washed with acetone and the eluent was then analyzed by GC-MS. From the chromatogram of the eluent in Fig. 8, besides DBT, two new sulfur species were detected at the retention times of 23.0 min and 23.4 min, respectively, which was confirmed to be DBTO and $DBTO_2$ by comparing the mass spectra of the new sulfur species with the standard mass spectra, as shown in Fig. 9. The above results demonstrate that in the presence of UV irradiation and $Ti_{0.5}Zr_{0.5}O_2$-500, DBT was oxidized to DBTO and $DBTO_2$, which were then selectively adsorbed on

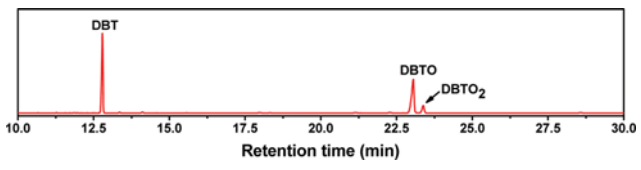

Fig. 8. Gas chromatogram of the eluent of the spent $Ti_{0.5}Zr_{0.5}O_2$-500 catalyst.

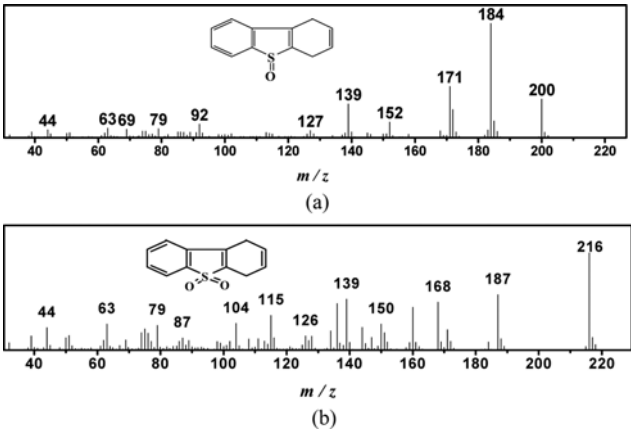

Fig. 9. Mass spectra of species at the retention time of 23.0 min (a) and 23.4 min (b) in Fig. 5, respectively.

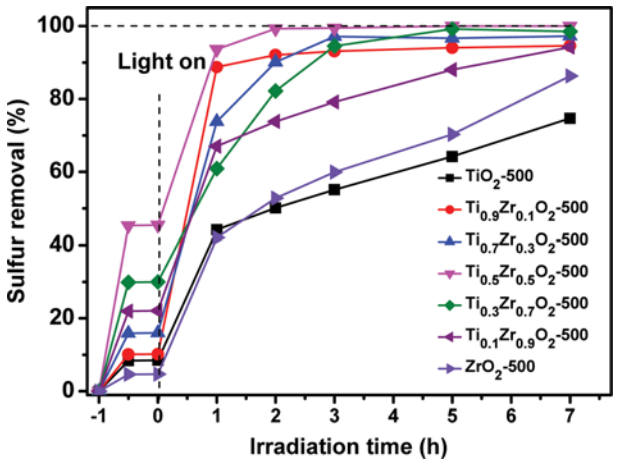

Fig. 11. The influence of the Ti/Zr molar ratio in $Ti_xZr_{(1-x)}O_2$-500 on its desulfurization performance with/without UV irradiation.

$Ti_{0.5}Zr_{0.5}O_2$-500. Note that organosulfur in model oil could not be oxidized in the presence of UV irradiation but without a photocatalyst (Fig. 7(c)); thus, it can be inferred that the oxidation of DBT occurred on $Ti_{0.5}Zr_{0.5}O_2$-500 under the UV irradiation. Moreover, no peroxides were detected in the model oil under UV irradiation with/without a photocatalyst, indicating air, rather than intermediates like hydroperoxides generated in-situ, served as the oxidant for sulfur oxidation [23]. That is, $Ti_{0.5}Zr_{0.5}O_2$-500 acted as a photocatalyst for photocatalytically oxidizing DBT to its corresponding sulfoxide and sulfone using air as the oxidant. However, no sulfoxides or sulfones were detected in the fuel samples (Fig. 7(d) and Fig. 7(e)) during the oxidation of DBT to DBTO and $DBTO_2$, indicating $Ti_{0.5}Zr_{0.5}O_2$-500 has strong adsorptive affinity for the produced sulfoxides and sulfones, probably due to the significantly increased polarity of the organosulfur molecule as the dipole magnitude increased from 1.364D for DBT to 4.425D for DBTO and 5.453D for $DBTO_2$ with the calculation by HyperChem 7.5. Therefore, the higher desulfurization capacity of $Ti_{0.5}Zr_{0.5}O_2$-500 in the presence of UV irradiation could be ascribed to the oxidation of the organosulfur compounds to the much more polar sulfoxides and sulfones, and $Ti_{0.5}Zr_{0.5}O_2$-500 has higher adsorptive affinity for the produced sulfoxides and sulfones than original organosulfur compounds due to the higher polarity of the former.

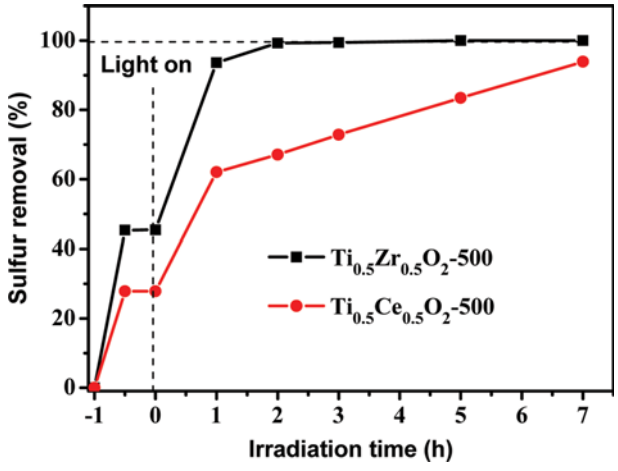

Fig. 10. Desulfurization performance of $Ti_{(1-x)}M_xO_2$ (M=Zr, Ce) with/without UV irradiation.

3. Desulfurization Performance of $Ti_{(1-x)}M_xO_2$ (M=Zr, Ce)

Fig. 10 shows the desulfurization performance of $Ti_{(1-x)}M_xO_2$ (M=Zr, Ce) with/without UV irradiation. Before UV irradiation, the adsorption equilibriums of DBT on both $Ti_{0.5}Zr_{0.5}O_2$-500 and $Ti_{0.5}Ce_{0.5}O_2$-500 were attained within 1 h. After UV irradiation was introduced, $Ti_{0.5}Zr_{0.5}O_2$-500 showed higher synergistic photocatalytic-adsorptive desulfurization performance, suggesting $Ti_{0.5}Zr_{0.5}O_2$-500 is a more promising bifunctional photocatalyst/adsorbent for desulfurization, which could be ascribed to the significantly higher surface area of the former.

4. Influence of the Ti/Zr Molar Ratio and Calcination Temperature of $Ti_xZr_{(1-x)}O_2$

Fig. 11 shows the influence of the Ti/Zr molar ratio in $Ti_xZr_{(1-x)}O_2$-500 on its desulfurization performance with/without UV irradiation. Before UV irradiation, the TiO_2-ZrO_2 mixed metal oxides exhibited higher adsorptive capacity for DBT than TiO_2 and ZrO_2 single oxides, probably due to the higher surface areas of the former, as listed in Table 1. Particularly, $Ti_{0.5}Zr_{0.5}O_2$-500 with the relatively higher surface area than any other $Ti_xZr_{(1-x)}O_2$-500 showed the highest adsorptive capacity for DBT. After UV irradiation was introduced, the sulfur removal significantly increased for both TiO_2 and ZrO_2 single oxides, suggesting both TiO_2 and ZrO_2 in TiO_2-ZrO_2 acted as the photcatalytic active sites and also the adsorptive sites for oxidized sulfur species. However, the TiO_2-ZrO_2 mixed metal oxides exhibited higher desulfurization capacity than TiO_2 and ZrO_2 single oxides, indicating the synergistic effect of TiO_2 and ZrO_2 in TiO_2-ZrO_2, probably due to the higher surface area of TiO_2-ZrO_2. Surprisingly, most of TiO_2-ZrO_2 mixed metal oxides, which had lower UV absorption (Fig. 3(a)), showed higher desulfurization capacity than TiO_2, suggesting UV absorption of TiO_2-ZrO_2 may not be the dominant factor affecting the synergistic photocatalytic-adsorptive desulfurization performance. For TiO_2-ZrO_2 mixed metal oxides with varying Ti/Zr molar ratio, $Ti_{0.5}Zr_{0.5}O_2$-500 showed the best desulfurization performance, by which nearly 100% of

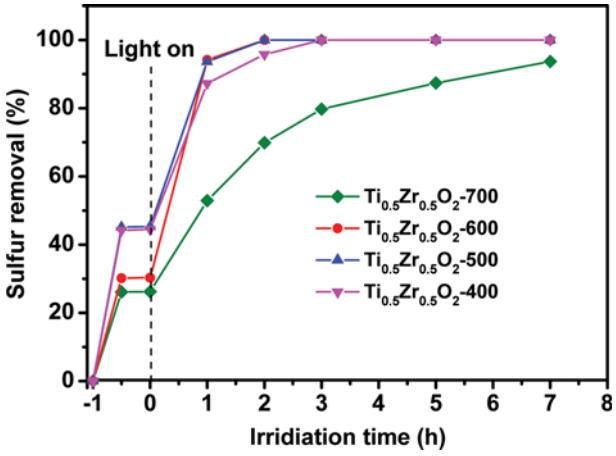

Fig. 12. The influence of the calcination temperature of $Ti_{0.5}Zr_{0.5}O_2$ on its desulfurization performance with/without UV irradiation.

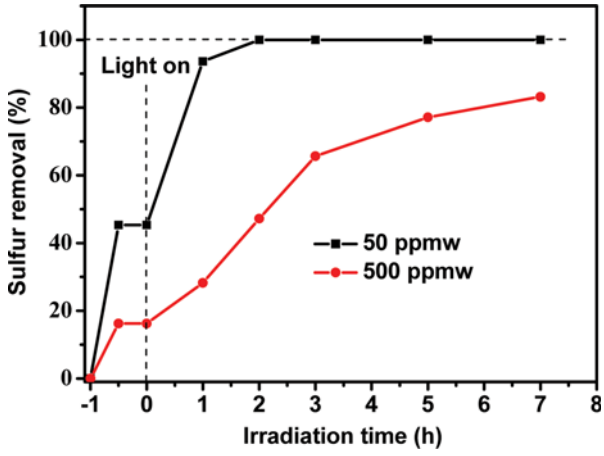

Fig. 13. Desulfurization performance of $Ti_{0.5}Zr_{0.5}O_2$-500 for model oils with the sulfur content of 50 ppmw and 500 ppmw, respectively.

sulfur removal was obtained at the UV irradiation time of 2 h.

Fig. 12 shows the influence of the calcination temperature of $Ti_{0.5}Zr_{0.5}O_2$ on its desulfurization performance with/without UV irradiation. Before UV irradiation, $Ti_{0.5}Zr_{0.5}O_2$-400 and $Ti_{0.5}Zr_{0.5}O_2$-500 showed similar adsorptive capacity for DBT, which was higher than those of $Ti_{0.5}Zr_{0.5}O_2$-600 and $Ti_{0.5}Zr_{0.5}O_2$-700, probably due to the higher surface areas of the former. After UV irradiation for 2 h, nearly 100% removal of sulfur was obtained over $Ti_{0.5}Zr_{0.5}O_2$-500 and $Ti_{0.5}Zr_{0.5}O_2$-600, which was higher than 95.8% and 69.9% for $Ti_{0.5}Zr_{0.5}O_2$-400 and $Ti_{0.5}Zr_{0.5}O_2$-700, indicating 500 °C and 600 °C were the optimal calcination temperarues for $Ti_{0.5}Zr_{0.5}O_2$. From the characterization results in Table 1, Fig. 2(b) and Fig. 3(b), the surface area of $Ti_{0.5}Zr_{0.5}O_2$ decreased with the calcination temperature, while the crystalline size and UV adsorption of $Ti_{0.5}Zr_{0.5}O_2$ increased with the calcination temperature. Therefore, the increase in desulfurization performance of $Ti_{0.5}Zr_{0.5}O_2$ with increasing the calcination temperature from 400 °C to 500 °C or 600 °C could be attributed to the increase in UV adsorption of $Ti_{0.5}Zr_{0.5}O_2$ with the calcination temperature, while the decrease in desulfurization performance of $Ti_{0.5}Zr_{0.5}O_2$ with increasing the calcination further to 700 °C could be ascribed to the sharp decrease in the surface area and increase in the crystalline size. Tailoring TiO_2-ZrO_2 with high surface area, high UV adsorption and small crystalline size could potentially lead to a photocatalyst/adsorbent with high desulfurization performance under UV irradiation.

5. Desulfurization Performance of $Ti_{0.5}Zr_{0.5}O_2$-500 for Model Oils Containing Different Sulfur Contents

To date, the sulfur content in real diesel fuel is still more than 500 ppmw in many parts of the world. To investigate the performance of the synergistic photocatalytic-adsorptive desulfurization process for relatively high-sulfur diesel fuel, the desulfurization of 500 ppmw-S model oil over $Ti_{0.5}Zr_{0.5}O_2$-500 under UV-irradiation was carried out, and the result is shown in Fig. 13. It was visible that the desulfurization rate of model oil containing 500 ppmw S was slower than that of model oil containing 50 ppmw S, and its sulfur removal reached 83.2% after reaction for 7 h with the fuel-to-$Ti_{0.5}Zr_{0.5}O_2$-500 weight ratio of 20, suggesting this process was

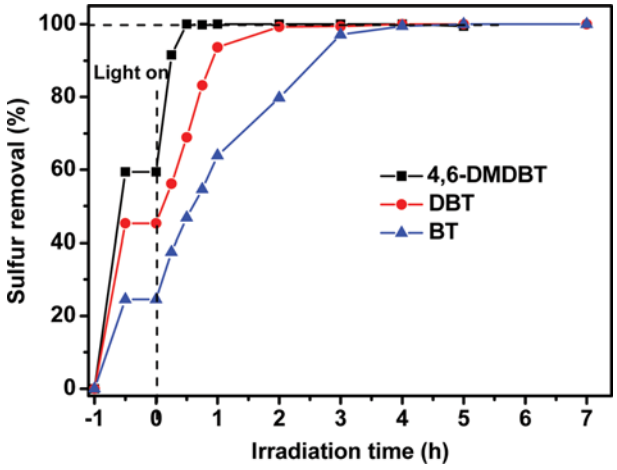

Fig. 14. The comparison of the synergistic photocatalytic-adsorptive desulfurization performance of $Ti_{0.5}Zr_{0.5}O_2$-500 for three different sulfur compounds.

less effective for model oil containing 500 ppmw S than that containing 50 ppmw S; however, the performance might be enhanced by improving the surface area of the catalyst/adsorbent or reducing the fuel-to-catalyst/adsorbent weight ratio, which will be addressed in our future work.

6. Removal of Different Organosulfur Compounds

Fig. 14 gives a comparison of the synergistic photocatalytic-adsorptive performance of $Ti_{0.5}Zr_{0.5}O_2$-500 for BT, DBT and 4,6-DMDBT. Before UV irradiation, the adsorptive selectivity of $Ti_{0.5}Zr_{0.5}O_2$-500 for different organosulfur compounds followed the order of 4,6-DMDBT>DBT>BT. After UV irradiation was introduced, nearly complete removal of BT, DBT and 4,6-DMDBT was achieved within 1 h, 2 h and 4 h of UV irradiation, respectively, indicating that the synergistic photocatalytic-adsorptive selectivity of $Ti_{0.5}Zr_{0.5}O_2$-500 for three organosulfur compounds also followed the order of 4,6-DMDBT>DBT>BT. Interestingly, the electron density on their sulfur atoms followed the same order of 4,6-DMDBT(5.760)>DBT(5.758)>BT(5.739) [24]. The reason for this

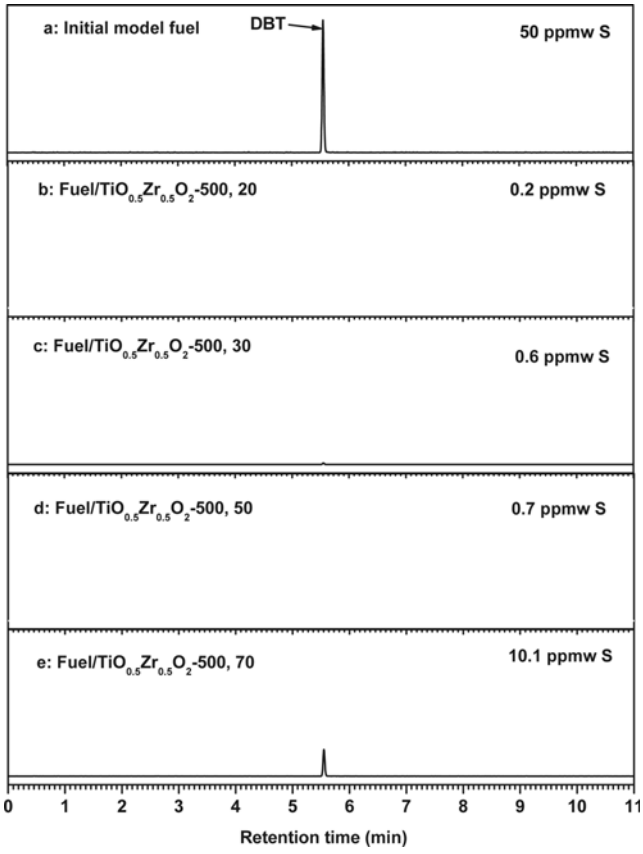

Fig. 15. Influence of the weight ratio of fuel to $TiO_{0.5}Zr_{0.5}O_2$-500 on the removal of DBT.

consistency may be that the sulfur atom with the higher electron density was more prone to be attacked by active oxygen involved in photocatalytic reaction. Also, the refractory dibenzothiophene and alkyl substituted dibenzothiophenes for the HDS process could be effectively removed by the synergistic photocatalytic-adsorptive over TiO_2-ZrO_2, which strongly suggests that the TiO_2-ZrO_2-based synergistic photocatalytic-adsorptive desulfurization process is a very promising technology for ultra-deep desulfurization of diesel fuel.

7. Influence of the Weight Ratio of Fuel to $TiO_{0.5}Zr_{0.5}O_2$-500

Fig. 15 shows the SCD chromatograms of the original model diesel fuel and the treated fuel by different amount of $TiO_{0.5}Zr_{0.5}O_2$-500 in the presence of UV irradiation for 2 h. When the fuel-to-$TiO_{0.5}Zr_{0.5}O_2$-500 weight ratio was increased from 20 to 50, the peak for DBT in the treated fuel could barely be seen, and the sulfur content could be decreased to below 1 ppmw. However, when the fuel-to-$TiO_{0.5}Zr_{0.5}O_2$-500 weight ratio reached 70, the peak for DBT appeared, and 10.1 ppmw of sulfur remained in model oil. It indicates that the maximum amount of model oil treated with 1 g of $TiO_{0.5}Zr_{0.5}O_2$-500 could reach 50 g with the ultimate sulfur content of less than 1 ppmw.

8. Influence of Aromatics on the Removal of Organosulfur

In adsorptive desulfurization, a relatively large amount of coexisting aromatics in diesel fuel has a strong inhibiting effect on the adsorption of organosulfur compounds due to their similar aromatic skeleton structures. To investigate the influence of aromatics in diesel on the desulfurization capacity of TiO_2-ZrO_2 in the presence of UV irradiation, a model oil containing 25 wt% toluene was prepared and taken for desulfurization test. Fig. 16 shows a comparison of sulfur removal of a toluene-containing model oil and a model oil without toluene in the presence of $Ti_{0.5}Zr_{0.5}O_2$-500 with/without the irradiation of UV light. It is visible that before irradiation, a sulfur removal of 45.2% was achieved in the model oil without toluene. In comparison, the sulfur removal sharply dropped to less than 2% when 25 wt% toluene was contained in the model oil, confirming the strong inhibiting effect of toluene on the adsorption of DBT. The toluene content in model oil after adsorption was then analyzed by GC-FID, and the toluene adsorption capacity on $Ti_{0.5}Zr_{0.5}O_2$-500 was found to be 72.2 mg/g, which was much higher than the sulfur adsorption capacity of 0.02 mg/g for the toluene-containing model diesel fuel. Interestingly, after UV irradiation was introduced, the sulfur removal of both model oils increased greatly due to the oxidation of DBT to DBTO and $DBTO_2$. After UV irradiation for 7 h, the sulfur removal of the toluene-containing fuel reached as high as 97.2%, which was only slightly lower than 99.6% of the model oil without toluene, demonstrating that the low adsorptive desulfurization selctivity of adosrptive process due to the strongly competitive adsorption of aromatics in diesel could be greatly improved by synergy of photocatalysis and adsorption of TiO_2-ZrO_2.

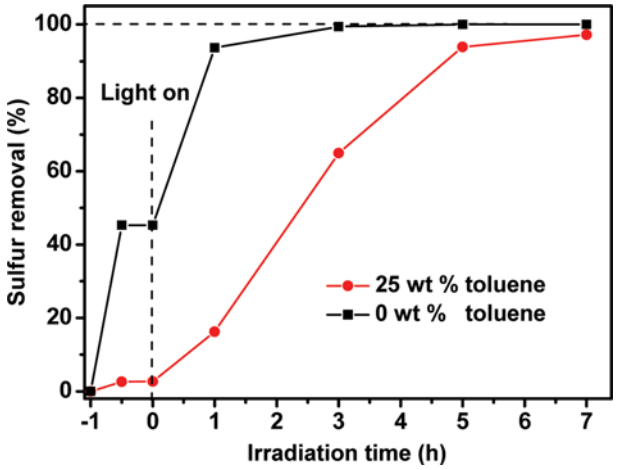

Fig. 16. The influence of toluene on the removal of dibenzothiophene using $Ti_{0.5}Zr_{0.5}O_2$-500 with/without UV irradiation.

9. Regeneration and Recycling of TiO_2-ZrO_2

For practical application, the regenerability and stability of a catalyst/adsorbent should be considered. The regeneration of TiO_2-ZrO_2 was conducted via acetonitrile washing followed by thermal treatment in air. Fig. 17 shows the recycling performance of TiO_2-ZrO_2 in a series of four consecutive desulfurization-regeneration cycles. It is visible that the performance of regenerated TiO_2-ZrO_2 was basically stable. Although it shows a slight decrease after 7 runs, the sulfur removal still retained over 95%, suggesting good regenerability of the TiO_2-ZrO_2.

10. The Possible Mechanism

From the above results and discussion, the synergistic photocat-

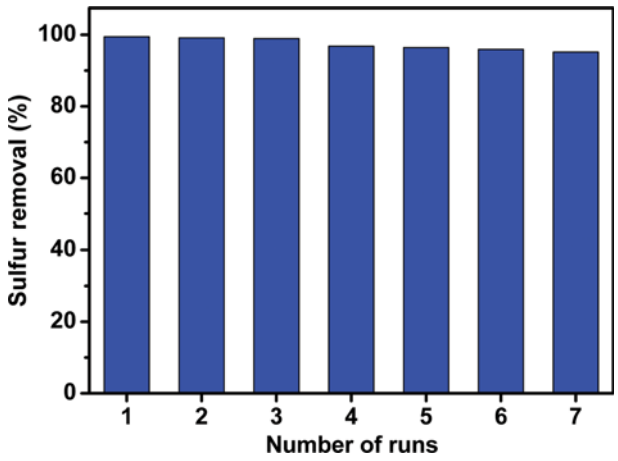

Fig. 17. Recycling runs of $Ti_{0.5}Zr_{0.5}O_2$-500 for synergistic photocatalytic-adsorptive desulfurization of model oil.

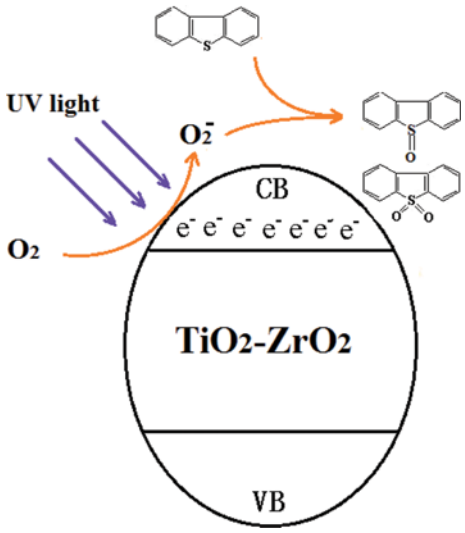

Fig. 18. Schematic diagram of synergistic photocatalytic-adsorptive desulfurization of model oil over TiO_2-ZrO_2.

alytic-adsorptive desulfurization mechanism can be proposed, and the scheme is shown in Fig. 18. When illuminated by UV light, the electrons of the valence band of TiO_2-ZrO_2 become excited and leap into the conduction band. The active electrons then activate the adsorbed molecular oxygen to produce superoxide anion (O_2^-) [11,12], which may bear selectivity towards organosulfur because the sulfur atom on organosulfur compounds has two unpaired electrons. Organosulfur compounds in diesel fuel were first oxidized by O_2^- to sulfoxides, which were further oxidized to sulfones. The produced polar sulfoxides and sulfones were then selectively adsorbed on the bifunctional material due to the much higher polarities of produced sulfoxides and sulfones than the original organosulfur compounds and other organic compounds in diesel fuel. Both TiO_2 and ZrO_2 in TiO_2-ZrO_2 acted as photocatalytic active sites and also the adsorptive sites for oxidized sulfur species, and the two types of active sites worked cooperatively to enhance the desulfurization capacity under UV irradiation.

CONCLUSION

Deep desulfurization of model oil by photocatalytic air oxidation and adsorption using $Ti_{(1-x)}M_xO_2$ (M=Zr, Ce) at ambient conditions was investigated. The UV irradiation greatly enhanced the adsorption of TiO_2-ZrO_2 for organosulfur in model oil, because under UV irradiation, TiO_2-ZrO_2 acted as both a photocatalyst and an adsorbent, over which organosulfur compounds were first photocatalytically oxidized to polar sulfoxides and sulfones over TiO_2-ZrO_2, which were then selectively adsorbed on the bifunctional material. The Ti/Zr molar ratio and calcination temperature were optimized to 5 : 5 and 500 °C with a sulfur removal of 99.6% after reaction for 2 h under UV irradiation. The low adsorptive desulfurization selctivity of adsorptive process due to the strongly competitive adsorption of aromatics in diesel could be greatly improved by employing the synergistic photocatalytic-adsorptive desulfurization process. The synergistic photocatalytic-adsorptive desulfurization performance of TiO_2-ZrO_2 for different organosulfur in diesel followed the order of 4,6-DMDBT>DBT>BT. TiO_2-ZrO_2 could be well regenerated by washing with acetonitrile followed by thermal treatment in air. Our findings provide a new perspective on ultra-deep desulfurization of diesel fuel.

ACKNOWLEDGEMENTS

This work was supported by the National Science Foundation of China (No. 21646003), the Talents Project of Beijing (No. 2014000020124G087), and the Undergraduate Research Program (No. 2016J00077).

REFERENCES

1. A. Stanislaus, A. Marafi and M. S. Rana, *Catal. Today*, **153**, 1 (2010).
2. C. Song and X. L. Ma, *Appl. Catal. B: Environ.*, **41**, 207 (2003).
3. M. Montazerolghaem, F. Seyedeyn-Azad and A. Rahimi, *Korean J. Chem. Eng.*, **32**, 328 (2015).
4. W. Zhang, H. Y. Liu, Q. B. Xia and Z. Li, *Chem. Eng. J.*, **209**, 597 (2012).
5. H. Y. Sun, L. P. Sun, F. Li and L. Zhang, *Fuel Process. Technol.*, **134**, 284 (2015).
6. L. M. Wu, J. Xiao, Y. Wu, S. K. Xian, G. Miao, H. H. Wang and Z. Li, *Langmuir*, **30**, 1080 (2014).
7. L. Qin, W. P. Shi, W. F. Liu, Y. Z. Yang, X. G. Liu and B. S. Xu, *Rsc Adv.*, **6**, 12504 (2016).
8. V. M. Bhandari, C. H. Ko, J. G. Park, S.-S. Han, S.-H. Cho and J.-N. Kim, *Chem. Eng. Sci.*, **61**, 2599 (2006).
9. X. L. Ma, A. N. Zhou and C. S. Song, *Catal. Today*, **123**, 276 (2007).
10. X. L. Ren, G. Miao, Z. Y. Xiao, F. Y. Ye, Z. Li, H. H. Wang and J. Xiao, *Fuel*, **174**, 118 (2016).
11. H. Saito and Y. Nosaka, *J. Phys. Chem. C*, **118**, 15656 (2014).
12. J. Z. Li, Y. Ma, Z. F. Ye, M. J. Zhou, H. Q. Wang, C. C. Ma, D. D. Wang, P. W. Huo and Y. S. Yan, *Appl. Catal. B: Environ.*, **204**, 224 (2017).
13. W. S. Zhu, Y. H. Xu, H. M. Li, B. L. Dai, H. Xu, C. Wang, Y. H. Chao and H. Liu, *Korean J. Chem. Eng.*, **31**, 211 (2014).
14. S. S. Chen, H. C. Hsi, S. H. Nian and C. H. Chiu, *Appl. Catal. B:*

Environ., **160**, 558 (2014).
15. D. F. Zhang and F. B. Zeng, *Appl. Surf. Sci.*, **257**, 867 (2010).
16. Q. Yuan, Y. Liu, L. L. Li, Z. X. Li, C. J. Fang, W. T. Duan, X. G. Li and C. H. Yan, *Micropor. Mesopor. Mater.*, **124**, 169 (2009).
17. M. Kobayashi and M. Flytzani-Stephanopoulos, *Ind. Eng. Chem. Res.*, **41**, 3115 (2002).
18. A. Kambur, G. S. Pozan and I. Boz, *Appl. Catal. B: Environ.*, **115**, 149 (2012).
19. C. S. Song, *Catal. Today*, **86**, 211 (2003).
20. X. L. Ma, L. Sun and C. S. Song, *Catal. Today*, **77**, 107 (2002).
21. X. L. Ma, M. Sprague and C. S. Song, *Ind. Eng. Chem. Res.*, **44**, 5768 (2005).
22. J. H. Kim, X. L. Ma, A. N. Zhou and C. S. Song, *Catal. Today*, **111**, 74 (2006).
23. R. Sundararaman, X. L. Ma and C. S. Song, *Ind. Eng. Chem. Res.*, **49**, 5561 (2010).
24. S. Otsuki, T. Nonaka, N. Takashima, W. H. Qian, A. Ishihara, T. Imai and T. Kabe, *Energy Fuels*, **14**, 1232 (2000).